Carbon dioxide UV laser-induced fluorescence in high-pressure flames

W.G. Bessler [a], C. Schulz [a,b,*], T. Lee [b], J.B. Jeffries [b], R.K. Hanson [b]

[a] *Physikalisch-Chemisches Institut, Ruprecht-Karls-Universität Heidelberg, Im Neuenheimer Feld 253, Heidelberg, 69120, Germany*
[b] *High Temperature Gasdynamics Laboratory, Mechanical Engineering Department, Stanford University, Stanford, CA 94305-3032, USA*

Abstract

Laser-induced fluorescence (LIF) of carbon dioxide is investigated with excitation between 215 and 255 nm with spectrally resolved detection in 5–40 bar premixed $CH_4/O_2/Ar$ and CH_4/air flat-flames at fuel/air ratios between 0.8 and 1.9. The LIF signal consists of a broad (200–450 nm) continuum with a faint superimposed structure, and this signal is absent in similar $H_2/O_2/Ar$ flames. There is strong evidence this signal arises from CO_2, as the signal variations with excitation wavelength, equivalence ratio and flame temperature all correlate with CO_2 absorption cross-sections. The signal is linear with pressure and laser fluence within the investigated ranges.
© 2003 Elsevier Science B.V. All rights reserved.

1. Introduction

Laser-based detection of combustion species has been proven an important tool for combustion research [1,2]. Many species require excitation at short UV wavelengths between 190 and 320 nm. Laser-induced fluorescence (LIF) of NO and OH are well-known examples, but other species are also detected in the UV; for example: optical absorption [3,4] and cavity ring-down [5] of CH_3, two-photon LIF of atoms [6], and UV–Raman and Rayleigh scattering [7]. In many practical applications attenuation of laser and signal light in this spectral range has been observed [8,9]. It was not until recently that the absorbing species were identified [10] as hot, vibrationally excited carbon dioxide (CO_2) and water (H_2O), based on measurements in engines [11] and high-pressure flames [12]. Quantitative temperature and wavelength-resolved absorption cross-sections were obtained from shock-tube experiments in a wide temperature and wavelength range [13]. The vacuum–UV absorption features of both species show a strong red-shift with increasing temperature. Relevant absorption cross-sections at flame temperatures extend to 230 nm for H_2O and 300 nm for CO_2. The fate of the excited molecules has not been previously characterized.

* Corresponding author. Fax: +49-6221-545050.
E-mail address: christof.schulz@pci.uni-heidelberg.de (C. Schulz).

The electronic structure of the CO_2 molecule [14,15] indicates that UV light absorption in the 200–300 nm range leads to population of the bent $^1B_2$ state 5.74 eV above ground state energy. This same excited state is also populated by the $CO(^1\Sigma^+) + O(^3P)$ recombination reaction which produces the so-called CO flame bands, identified by Dixon [16], via intersystem crossing.

Photodissociation of hot H_2O and CO_2 is well-known after excitation at 193 nm [17,18]. First indications show that at longer wavelengths, H_2O and CO_2 photodissociation also occur [19–21]. This is especially relevant for H, O, and CO two-photon diagnostics where focused laser light in the 200–230 nm range is used and photodissociation of the major combustion products might lead to the production of interference quantities of the target species.

Here we identify the laser-induced fluorescence of CO_2 by systematic studies in high-pressure methane flames at pressures up to 40 bar. To separate the broadband CO_2-LIF signal from signal contributions of other species, nitrogen-free flames (diluted with Ar) were also studied. LIF of hot O_2 was minimized by tuning the laser wavelength to minima in the O_2 absorption spectrum. Hydrogen/oxygen/argon flames were investigated to demonstrate the absence of the broadband emission signal we attribute to CO_2. The dependence of CO_2-LIF on temperature and excitation wavelength compares well with the magnitude of the CO_2 absorption. Finally, the intensity of CO_2 fluorescence is compared to the signal intensity of nitric oxide LIF. Work to quantify the LIF quantum yield is underway.

2. Experimental

Laminar, premixed methane/air, methane/oxygen/argon and hydrogen/oxygen/argon flat-flames at pressures from 1 to 40 bar were stabilized on a porous, sintered stainless steel plate of 8 mm diameter. This burner was mounted in a stainless steel housing with an inner diameter of 60 mm with pressure stabilization ±0.1 bar [22]. Optical access to the flame was possible via four quartz windows. Investigations were performed for fuel/air equivalence ratios of $\phi = 0.8$–1.9. The soot limit was found between $\phi = 1.8$ and 1.9 for the $CH_4/O_2/Ar$ flame at 20 bar.

A Nd:YAG-pumped (Quanta Ray GCR250) frequency-doubled (BBO) dye laser (LAS, LDL205) was used to produce laser light (ca., 1 mJ, 0.4 cm^{-1} full-width at half maximum (FWHM)). The laser was tuned to different excitation wavelengths. The wavelengths were selected from O_2-LIF simulations [23,24] for minimum O_2-LIF interference. The laser was scanned in a 0.5-nm range around the simulated O_2 minima to get the experimental minima. Three different laser dyes were necessary to cover the broad excitation wavelength range of 40 nm. Measurements were carried out at 215.70, 220.88, and 226.07 nm (Coumarin 120); 233.65, 235.88, and 242.15 nm (Coumarin 102); 247.95, 251.69, and 255.88 nm (Coumarin 307). The laser beam quality changes slightly within the investigated wavelength range. Therefore, O_2-Raman signals and their known wavelength dependence are measured in the cold fresh gas and used as an internal reference.

The laser beam was aligned parallel to the burner surface and passed through the center of the flame 2 mm above the burner matrix. The pulse energy was measured with a fast photodiode (LaVision). The beam was mildly focused with a spherical lens ($f = 700$ mm), and the measurement occurs in the beam waist. Fluorescence signals were collected at right angles to the laser beam and focused with a $f = 105$ mm, $f_\# = 4.5$ achromatic UV lens (Nikon) onto the horizontal entrance slit of a $f = 250$ mm imaging spectrometer (Chromex 250IS, 300 grooves/mm grating, blazed for 300 nm operated in first order). Narrowband dielectric mirrors (FWHM ~15 nm) were used to suppress elastically scattered laser light. The spectrally dispersed signal was detected with an intensified CCD camera (LaVision DynaMight III). Each laser pulse yielded a complete fluorescence spectrum maintaining one-dimensional spatial resolution along the laser light path. In these images the central area of the flame where temperature and concentrations are homogeneous was then chosen and integrated over the spatial axis, yielding a fluorescence spectrum.

Corrections to the signal for spectral response of filter, spectrometer and camera were made using

calibration measurements with a calibrated D_2-lamp (Optronics Laboratories). In order to compare signal intensities for different wavelength excitation (with slight variations in beam quality and beam alignment), O_2-Raman scattering intensities at 20 bar in the cold coflow region were used as an internal reference while accounting for the wavelength-dependence of Raman cross-sections. CO_2-LIF signals were averaged on the spectral axis to simulate different detection bandpass filters (280–320 nm and 320–370 nm, respectively). In lean flames O_2-LIF contribute to the signal transmitted by the shorter-wavelength bandpass.

3. Results

In high-pressure flames, pressure-induced line broadening makes it difficult to completely avoid the excitation of strongly fluorescing species like NO and hot O_2 by tuning the laser wavelength off-resonance. Therefore, comparison measurements were made by eliminating nitrogen using oxygen diluted in argon (20/80 volume ratio; note this dilution retains a similar heat capacity to undiluted methane/air flames and thus temperatures similar to the flames studied in [25]). In these flames, the excitation wavelengths were selected to minimize oxygen excitation. Even so, O_2-LIF dominates the emission spectrum in lean and stoichiometric flames at high pressure (Fig. 1, $\phi = 0.8$). Underlying the oxygen spectrum is a broad-band background that can be observed without O_2-LIF contribution in the fuel rich ($\phi = 1.1$ and 1.4) flames. This signal is attributed to CO_2-LIF. In the very rich flame ($\phi = 1.8$) additional strong signal from soot precursors (polycyclic aromatic hydrocarbons, PAH) is observed which has a qualitatively different spectral shape. The PAH-LIF spectra have a maximum at longer wavelength relative to the broadband CO_2-LIF emission spectrum. When carbon-containing fuel is replaced by hydrogen, the broadband signal disappears completely (lower diagram in Fig. 1).

To assure the assignment of the broadband fluorescence as CO_2-LIF, the signal dependence on CO_2 concentration, temperature, and excitation wavelength is investigated and compared to the
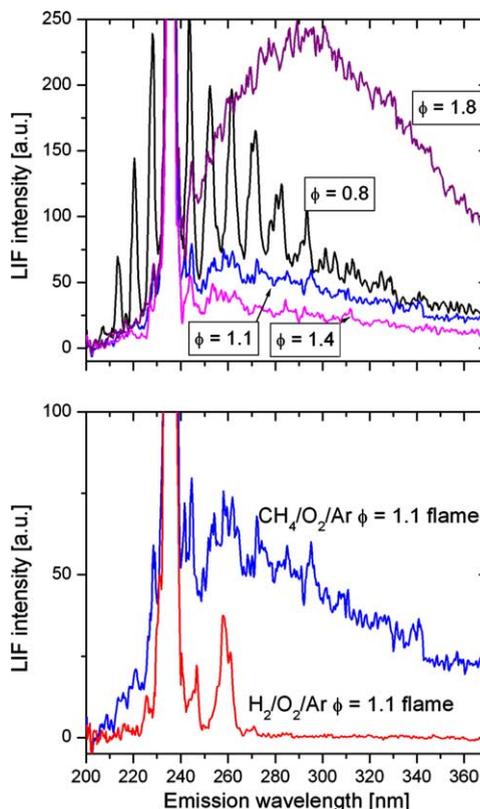

Fig. 1. Upper diagram: Emission spectra with 235.88-nm excitation in the 20-bar $CH_4/O_2/Ar$-flame with $\phi = 0.8$, 1.1, 1.4 and 1.8. The strong signal at 236 nm is elastically scattered laser light; the line spectrum at $\phi = 0.8$ is the vibrational progression of O_2 B–X transitions. Lower diagram: Emission spectra with 235.88-nm excitation in $CH_4/O_2/Ar$ (upper trace) and $H_2/O_2/Ar$ (lower trace) flame. 20 bar, $\phi = 1.1$. Note the peak near 260 nm in the $H_2/O_2/Ar$ flame corresponds to Raman scattering from H_2O. The signal is accumulated over 1000 laser pulses.

variation expected from the recently determined CO_2 absorption cross-sections [13].

The CO_2-fluorescence signal is strongly dependent on excitation wavelength (Fig. 2). This is in qualitative agreement with the wavelength dependence of the CO_2 absorption cross-section. We make the zeroth-order assumption that the fluorescence quantum yield is independent of temperature and that the CO_2-LIF signal is proportional to the absorption cross-sections. The wavelength-dependence of the absorption cross-section yields estimates for the temperature based on the data in
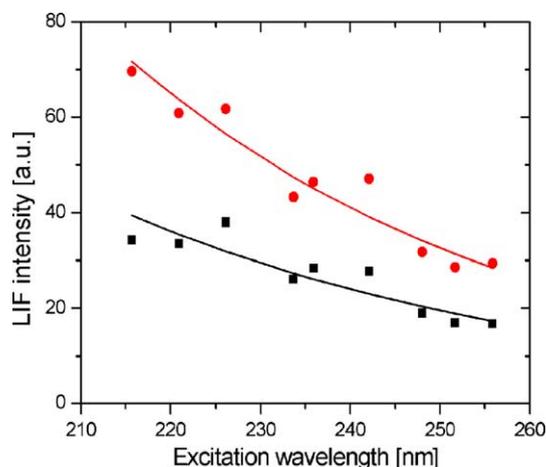
Fig. 2. Wavelength-dependent CO_2-LIF intensities at 20 bar, fuel/air equivalence ratio $\phi = 1.1$ for 280–320 nm and 320–370 nm bandpass (disks and rectangles resp.). The fit assumes wavelength-independent fluorescence quantum yields and estimates the gas temperature based on the temperature-dependent CO_2 absorption cross-section (4480 and 4320 K, resp.).

[13]. The inferred temperature is well above 4000 K. This indicates that the assumption of wavelength-independent fluorescence quantum yield is not valid. Experiments to measure the local temperature are underway, and this data will enable determination of the wavelength-dependence of the quantum yield.

The equivalence ratio determines both local temperature and CO_2 number density. Both quantities can be calculated for the post-flame region of the premixed flame based on the assumption of chemical equilibrium and adiabatic flame temperatures [26]. The results are shown in Fig. 3. Combining these results with the strongly temperature and wavelength-dependent CO_2 absorption cross-section allows calculation of the local CO_2 absorbance. With the zeroth-order assumption that the CO_2 fluorescence yield is independent of temperature and gas composition and that adiabatic equilibrium calculations describe the local flame conditions accurately, the measured fluorescence should be directly proportional to CO_2 absorbance. A more detailed analysis of these assumptions based on flame temperature measurements is under way and will be presented in a forthcoming publication.
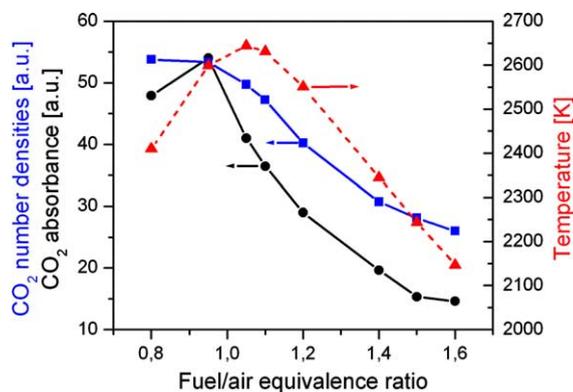

Fig. 3. Adiabatic flame temperatures (triangles), calculated CO_2 number densities (squares) and resulting CO_2 absorbance (disks) number densities in dependence on equivalence ratio in the $CH_4/O_2/Ar$ flame.

Fig. 4 shows that the CO_2-LIF intensity correlates well with the CO_2 absorbance. However, there remains a systematic variation. For all investigated excitation wavelengths, lean flames give stronger CO_2-LIF signal than the respective rich flames with the same CO_2 absorbance. Temperature measurements in the flames are under way to eliminate the potential error from assuming adiabatic flame temperatures. These measurements will
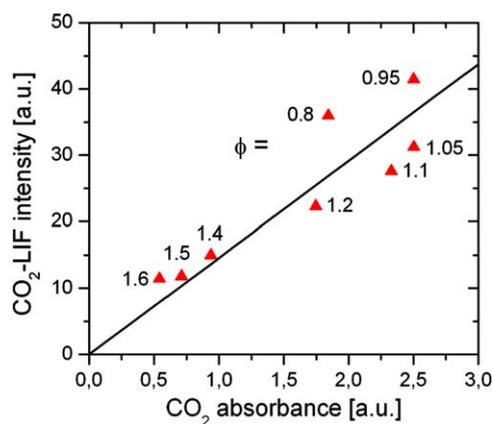

Fig. 4. CO_2-LIF intensity (320–370-nm bandpass) versus CO_2 absorbance (calculated from CO_2 number density and temperature-dependent absorption cross-section) for 235.88-nm excitation. The symbols represent measurements at different equivalence ratios ϕ; the linear fit represents the case of invariant fluorescence quantum yield for all conditions.

then allow an evaluation of the T-variation in fluorescence quantum yields.

For practical considerations the response of CO_2 fluorescence signal on pressure and laser fluence is of interest. The CO_2 fluorescence signal is linear with laser pulse energy in the 20–700 μJ range (approximately 0.7–26 MW/cm^2) that was accessible with our dye-laser system. The CO_2-LIF signal also increases linearly with pressure in the 1–40 bar range. This indicates that the fluorescence lifetime is not limited by fluorescence quenching in the respective pressure range. We expect that dissociation and fast intersystem crossing (ISC) of the excited CO_2 are the lifetime-determining processes. This, however, means that CO_2 LIF might become an important interference in high-pressure LIF diagnostics of species that are strongly affected by collisional quenching (like NO). LIF interference for a species with a quenching-dominated quantum yield by LIF from another species whose fluorescence lifetime is limited by fast non-collisional processes causes the signal-to-background ratio to deteriorate linearly with pressure.

Fig. 5 shows an example for NO diagnostics in a $\phi = 0.83$ CH_4/air flame at 60 bar with NO A-X(0,2) O_{12}-bandhead excitation at 247.94 nm [27]. The flame is doped with 300 ppm NO. The NO and O_2 fluorescence lines are superimposed on a significant broadband emission of CO_2-fluorescence. Under these conditions, CO_2 becomes a source for strong signal interference. A quantitative analysis for various flame conditions is given in [27] using spectral simulations for the NO and O_2-LIF contributions [23].

4. Summary

We investigated broadband laser-induced fluorescence after excitation in the 215–255-nm range in various flames at elevated pressures. There is strong evidence that the broadband fluorescence signal in the 200–450-nm range observed in rich, stoichiometric and lean hydrocarbon flames after laser excitation in the 225–250-nm range can be attributed to CO_2-LIF. This signal completely disappears in carbon-free flames. The signal is clearly distinguishable from LIF emission of polycyclic aromatic hydrocarbons that appears in very rich flames only. The excitation-wavelength dependence is similar to that of the absorption cross-section. While the temperature dependence of LIF intensities shows only minor deviations from the correlation with absorption cross sections, a systematic variation of the fluorescence quantum yield seems to be present with different excitation wavelengths.

The CO_2-LIF increases linearly with pressure, making CO_2 a potential source of interference in high-pressure detection of collisionally quenched species. In turn, CO_2 fluorescence might open up new opportunities for diagnostics for isothermal high-pressure mixing processes or for temperature in high-pressure systems with constant CO_2 concentration.

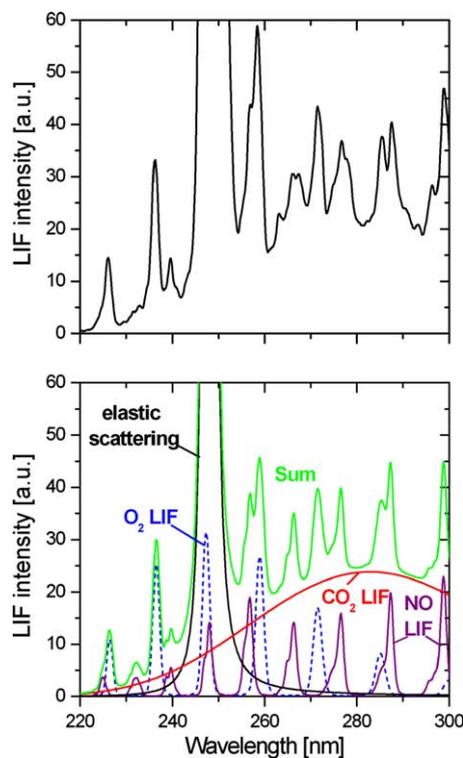Experiments are underway to measure the temperature field in the flames studied here. These

Fig. 5. Premixed flat methane/air flame: 60 bar, $\phi = 0.83$, 300 ppm NO seed. The experimental data (upper panel) are compared to simulations of NO, O_2, and CO_2-LIF (lower panel). The signal is accumulated over 50 laser pulses.

results will enable us to quantify the temperature and wavelength-dependence of the CO_2 fluorescence quantum yield.

References

[1] K. Kohse-Höinghaus, J.B. Jeffries, Applied Combustion Diagnostics, Taylor and Francis, New York, 2002.

[2] J. Wolfrum, Proc. Combust. Inst. 27 (1998) 1.

[3] T. Etzkorn, J. Fitzer, S. Muris, J. Wolfrum, Chem. Phys. Lett. 208 (1993) 307.

[4] D.F. Davidson, A.Y. Chang, M.D. DiRosa, R.K. Hanson, J. Quant. Spectrosc. Radiat. Transfer 49 (1993) 559.

[5] P. Zalicki, Y. Ma, R.N. Zare, J.R. Dadamio, E.H. Wahl, T.G. Owano, C.H. Kruger, Chem. Phys. Lett. 234 (1995) 269.

[6] W.K. Bischel, B.E. Perry, D.R. Crosley, Chem. Phys. Lett. 82 (1981) 85.

[7] R.W. Pitz, J.A. Wehrmeyer, J.M. Bowling, T.S. Cheng, Appl. Opt. 29 (1990) 2325.

[8] M. Knapp, A. Luczak, H. Schlüter, V. Beushausen, W. Hentschel, P. Andresen, Appl. Opt. 35 (1996) 4009.

[9] F. Hildenbrand, C. Schulz, V. Sick, E. Wagner, Appl. Opt. 38 (1999) 1452.

[10] C. Schulz, J.B. Jeffries, D.F. Davidson, J.D. Koch, J. Wolfrum, R.K. Hanson, Proc. Comb. Inst. 29 (2002) 2725.

[11] F. Hildenbrand, C. Schulz, Appl. Phys. B 73 (2001) 165.

[12] W.G. Bessler, C. Schulz, T. Lee, D.I. Shin, M. Hofmann, J.B. Jeffries, J. Wolfrum, R.K. Hanson, Appl. Phys. B 75 (2002) 97.

[13] C. Schulz, J.D. Koch, D.F. Davidson, J.B. Jeffries, R.K. Hanson, Chem. Phys. Lett. 355 (2002) 82.

[14] J.W. Rabalais, J.M. McDonald, V. Scherr, S.P. McGlynn, Chem. Rev. 71 (1971) 73.

[15] A. Spielfiedel, N. Feautrier, C. Cossart-Magos, G. Chambaud, P. Rosmus, H.-J. Werner, P. Botschwina, J. Chem. Phys. 97 (1992) 8382.

[16] R.N. Dixon, Discuss. Faraday Soc. 35 (1963) 105.

[17] D. Häusler, P. Andresen, R. Schinke, J. Chem. Phys. 87 (1997) 3949.

[18] M. Koshi, M. Yoshimura, H. Matsui, Chem. Phys. Chem. 176 (1991) 519.

[19] A.P. Nefedov, V.A. Sinel'shchikov, A.D. Usachev, A.V. Zobnin, Appl. Opt. 37 (1998) 7729.

[20] J.E.M. Goldsmith, Opt. Lett. 11 (1986) 416.

[21] T.B. Settersten, A. Dreizler, B. Patterson, P. Schrader, R.L. Farrow, Appl. Phys. B 76 (2003) 479.

[22] W.G. Bessler, C. Schulz, T. Lee, J.B. Jeffries, R.K. Hanson, Appl. Opt. 41 (2002) 3547.

[23] W.G. Bessler, C. Schulz, V. Sick, J.W. Daily, A versatile modeling tool for nitric oxide LIF spectra, 3rd Joint Meeting of the US Sections of the Combustion Institute, Chicago, 2003.

[24] W.G. Bessler, T. Lee, C. Schulz, J.B. Jeffries, R.K. Hanson, UV laser-induced fluorescence of carbon dioxide in high-pressure flames, 3rd Joint Meeting of the US Sections of the Combustion Institute, Chicago, 2003.

[25] T. Lee, J.B. Jeffries, R.K. Hanson, W.G. Bessler, C. Schulz, Quantitative NO-LIF Temperature Imaging in High-Pressure Flames, 41st AIAA Aerospace Sciences Meeting and Exhibit, January 6–9, Reno, NV, 2003, p. Paper No. 2003.

[26] D.G. Goodwin, Thermochemical calculator (TCC), http://blue.caltech.edu/tcc.

[27] W.G. Bessler, C. Schulz, T. Lee, J.B. Jeffries, R.K. Hanson, Appl. Opt. (2003) in press.